Multi-indicator Inference Scheme for Fuzzy Assessment of Power System Transient Stability

Tingjian Liu, Youbo Liu, *Member, IEEE*, Junyong Liu, *Member*, *CSEE*, Yue Yang, Gareth A. Taylor, *Senior Member, IEEE*, and Zhengwen Huang

***Abstract*—A multi-indicator inference scheme is proposed in this paper to achieve an intuitive assessment of post-fault transient stability of power systems. The proposed scheme uses the fuzzy inference technique to classify the stability level as "safe," "low-risk," "high-risk," and "danger." A multi-criteria quality assessment method is first introduced. Several transient indicators are then proposed as assessment criteria. To select the effective indicators for assessment, correlation mining using univariate regression analysis is performed between each indicator and a critical clearance time (CCT)-based stability index. The fuzzy sets of indicators for different stability levels are then determined according to their correlations with the stability index. The weighting factors of indicators are also allocated according to their regression error in correlation mining. The proposed inference scheme is further demonstrated and its effectiveness is validated in case studies on IEEE 68-bus system and a 756-bus transmission system in China.**

***Index Terms*—Fuzzy assessment, multi-criteria assessment, transient indicators, transient stability awareness.**

I. Introduction

TRANSIENT stability refers to the ability of power systems to maintain synchronism when subjected to severe disturbances [1]. Online awareness of transient stability is essential to system operations since this allows for prediction of insecurity, whereby control schemes are implemented in a timely fashion to prevent system collapse and blackout.

Time domain simulation (TDS) provides detailed power system post-fault responses; however, TDS is computationally intensive and cannot achieve online awareness. In recent years pattern recognition methods have been widely used to fulfill online transient stability awareness. Lasso is used for prediction of the transient stability boundary of a given fault contingency [2]. In order to realize robust online dynamic security assessment, ensemble decision trees (DTs) are used for mitigating inaccurate classifications caused by missing phasor measurement unit (PMU) measurements and system topology changes respectively in [3] and [4]. A systematic approach for dynamic security assessment and preventive control based on DTs is proposed in [5]. In [2]–[5], state variables of pre-fault conditions are employed as input features. Post-fault responses can be obtained in real time by the employment of wide-area measurement system (WAMS), thus application of pattern recognition methods with post-fault features has become another emerging research trend. In [6], a support vector machine (SVM)-based classifier is trained for the prediction of rotor angle instability. This SVM-based classifier employs similarity estimations of post-fault voltage trajectories to pre-identify template features as input. In addition, post-fault trajectories of generators and transient energy features are also separately employed as input features of SVM-based classifiers, as described in [7] and [8]. A DT-based classifier fed with post-fault parameters is presented in [9].

The pattern recognition-based assessment methods described above can predict the stability status of a post-fault system; however, they cannot inform system operators how stable the system is. Compared with quantitative evaluation of stability margin, linguistically fuzzy stability levels, such as "safe," "low-risk," "high-risk," and "danger," are more comprehensive to system operators. Hence fuzzy assessment method is utilized for online awareness of transient stability level in this paper. There are a number of fuzzy techniques available for stability assessment in the literature. In [10], a mapping rule of stability level against pre-fault operating variables is used to achieve online awareness of stability level. A three-stage fuzzy inference strategy is proposed in [11] for assessment of dynamic security level. A novel method that combines a quality assessment model and entropy-based criterion weighting is applied in [12] for fast fault contingency screenings.

In this paper, a multi-indicator inference scheme is proposed for fast inference of post-fault transient stability levels of power systems. A multi-criteria quality assessment method is first introduced. A set of transient indicator is then proposed as criteria to assess transient stability. A feature selection method based on correlation mining is further applied to choose effective indicators for multi-indicator assessment. The correlations between indicators and a critical clearance time (CCT)-based stability margin index are tested through offline training. The value ranges of these indicators are then divided into four fuzzy stability levels of "safe," "low-risk," "high-

Manuscript received December 4, 2015; revised April 27, 2016 and June 27, 2016; accepted July 27, 2016. Date of publication September 30, 2016; date of current version July 27, 2016. This work was supported in part by the National Natural Science Foundation of China (NSFC Project, No. 51437003 and No. 51261130472).

T. Liu, Y. Liu (corresponding author, e-mail: liuyoubo@scu.edu.cn), J. Liu, and Y. Yang are with the School of Electrical Engineering and Information, Sichuan University, Chengdu 610065, China.

G. Taylor and Z. Huang are with Electronic and Computer Engineering Brunel University, London, UB8 3PH, UK.

DOI: 10.17775/CSEEJPES.2016.00029

risk," and "danger," according to the correlation functions. Meanwhile, the weighting factors for all the indicators are determined by the regression error of their own correlation functions. Then the procedure of the proposed inference scheme is demonstrated in detail. The effectiveness of this proposed awareness scheme is subsequently verified via case studies on IEEE 68-bus system and a 756-bus transmission system in China.

The rest of this paper is organized as follows. The multi-criteria fuzzy assessment method based on quality assessment is described in Section II. Transient indicators used as stability criteria and the correlation-based indicator selection approach are presented in Section III. The proposed multi-indicator inference scheme is demonstrated in Section IV. Case study on IEEE 68-bus system is presented to illustrate the effectiveness of the proposed scheme in Section V. Application to a practical transmission system is provided in Section VI. Conclusions are drawn in Section VII.

II. Multi-criteria Fuzzy Assessment Methodology

In this section, multi-criteria quality assessment method is introduced. For simplicity, the term "criterion" is replaced by "transient indicators" while "quality" is changed to "stability level" in the description of the method.

$TI = \{TI_n\}_{n=1\ldots N}$ is a set of transient indicators to evaluate transient stability level. $E = \{e_n\}_{n=1\ldots N}$ is the evaluation of a post-fault system stability according to *TI*. If $(C_1, C_2, \ldots, C_K)$ are fuzzy sets for K stability levels, then the value range of each indicator should be divided into K intervals ($C_{n1} \in [a_{n0} - a_{n1}], C_{n2} \in [a_{n1} - a_{n2}], \ldots, C_{nK} \in [a_{nK-1} - a_{nK}]$), where $a_{n0} < a_{n1} < \ldots < a_{nK}$.

e_n is the quantitative evaluation according to the n^{th} indicator TI_n. μ_{nk} is the probabilistic membership in which e_n belongs to the k^{th} stability level. Equations (1) and (2) should be always satisfied.

$$\mu_k \geq 0, \ \sum_{k=1}^{K} \mu_k = 1 \tag{1}$$

$$\mu_{nk} \geq 0, \ \sum_{k=1}^{K} \mu_{nk} = 1 \tag{2}$$

For any stability level $C_k (k = 1, 2, \ldots, K)$, given that

$$b_{nk} = (a_{nk-1} + a_{nk})/2,$$
$$d_{nk} = \min(|b_{nk} - a_{nk}|, |b_{nk+1} - a_{nk}|),$$

the membership μ_{nk} can be calculated based on the trapezoid shaped membership function. The membership function $\mu_{n1}(e_n)$ for the first fuzzy set C_{n1} is shown by (3).

$$\mu_{n1}(e_n) = \begin{cases} 1, & e_n < a_{n1} - d_{n1}; \\ |e_n - a_{n1} - & a_{n1} - d_{n1} \leqslant e_n \\ d_{n1}|/2d_{n1}, & \leqslant a_{n1} + d_{n1}; \\ 0, & a_{n1} + d_{n1} < e_n. \end{cases} \tag{3}$$

The membership function $\mu_{nK}(e_n)$ for the last fuzzy set C_{nK} is shown by (4).

$$\mu_{nK}(e_n) = \begin{cases} 1, & a_{nK-1} + d_{nK-1} < e_n; \\ |e_n - a_{nK-1} - & a_{nK-1} - d_{nK-1} \leqslant e_n \\ d_{nK-1}|/2d_{nK-1}, & \leqslant a_{nK-1} + d_{nK-1}; \\ 0, & e_n < a_{nK-1} - d_{nK-1}. \end{cases} \tag{4}$$

And the membership function $\mu_{nk}(e_n)$ for the other fuzzy set $C_{nk} (k = 2, 3, \ldots, K-1)$ is shown by (5).

$$\mu_{nk}(e_n) = \begin{cases} 0, & e_n < a_{nk-1} - d_{nk-1}; \\ |e_n - a_{nk-1} + & a_{nk-1} - d_{nk-1} \leqslant e_n \\ d_{nk-1}|/2d_{nk-1}, & \leqslant a_{nk-1} + d_{nk-1}; \\ 1, & a_{nk-1} + d_{nk-1} < e_n \\ & < a_{nk} + d_{nk}; \\ |e_n - a_{nk} + & a_{nk} - d_{nk} \leqslant e_n \\ d_{nk}|/2d_{nk}, & \leqslant a_{nk} + d_{nk}; \\ 0, & a_{nk} + d_{nk} < e_n. \end{cases} \tag{5}$$

Then the membership μ_k in which transient stability is classified as the k^{th} fuzzy set can be computed by (6)

$$\mu_k = \sum_{n=1}^{N} w_n \mu_{nk}, \ \exists w_n > 0, \ \sum_{n=1}^{N} w_n = 1 \tag{6}$$

where w_n is the weighting factor for the n^{th} criterion.

Given that λ is the credibility measurement and (7) is satisfied,

$$k_0 = \min\{k | \sum_{l=1}^{k} \mu_{xl} \geq \lambda, 1 \leq k \leq K\}. \tag{7}$$

The transient stability level of the post-fault system can be classified into fuzzy set C_{k0}. In this paper, λ is defined as 0.6.

III. Transient Indicators and Correlation-based Indicator Selection

A. Transient Indicators

Several types of severity indices have been proposed for dynamic security assessment (DSA) or transient stability assessment (TSA) in the literature. Integral square generator angle index (*ISGA*) is used to assess the transient coherency of generators in [13]. Fuzzy dynamic security indices (*FDSI*) assess the dynamic security level in [11]. Frequency-domain-based wide-area severity indices (*WASI*) assess dynamic vulnerability in [14]. The pair-wise potential energy index of generators is used in [15] to determine the set of critical generators. In this paper, thirteen types of transient indicators are proposed to assess the stability of post-fault systems, as shown in Table I.

δ and ω are the power angle and rotor speed of generators; P_{m} and P_{e} are the mechanical power input and electrical power output of generators; and V is the voltage magnitude of a generator's integration bus. Assuming that PMUs are installed at all the integration buses, for online application, δ and ω can be approximated by the phase angle and angular frequency of integration buses; and P_{e} can be approximated by the active power flow of step-up transformers. Considering

TABLE I
TRANSIENT INDICATORS

No.	Transient Indicator	Equation
1	Separation of generator power angle under COI reference at fault clearance time	$TI_1 = \left\|\delta_i^{\mathrm{COI}}(t_{\mathrm{cl}})\right\| = \left\|\delta_i(t_{\mathrm{cl}}) - \delta_{\mathrm{COI}}(t_{\mathrm{cl}})\right\|$
2	Maximum generator power angle separation at fault clearance time	$TI_2 = \max_{i,j\in G} \left\|\delta_i(t_{\mathrm{cl}}) - \delta_j(t_{\mathrm{cl}})\right\|$
3	Integral square generator angle index (ISGA) [13]	$TI_3 = \frac{1}{N_{\mathrm{G}}} \int_{t_{\mathrm{cl}}}^{t_{\mathrm{end}}} \sum_{i=1}^{N_{\mathrm{G}}} (\delta_i - \delta_{\mathrm{COI}})^2 \mathrm{d}t$
4	Separation of generator rotor speed under COI reference at fault clearance time	$TI_4 = \left\|\omega_i^{\mathrm{COI}}(t_{\mathrm{cl}})\right\| = \left\|\omega_i(t_{\mathrm{cl}}) - \omega_{\mathrm{COI}}(t_{\mathrm{cl}})\right\|$
5	Maximum generator rotor speed separation at fault clearance time	$TI_5 = \max_{i,j\in G} \left\|\omega_i\left(t_{\mathrm{cl}}\right) - \omega_j\left(t_{\mathrm{cl}}\right)\right\|$
6	Integral square generator speed index (ISGS)	$TI_6 = \frac{1}{N_{\mathrm{G}}} \int_{t_{\mathrm{cl}}}^{t_{\mathrm{end}}} \sum_{i=1}^{N_{\mathrm{G}}} (\omega_i - \omega_{\mathrm{COI}})^2 \mathrm{d}t$
7	Accelerating rate of generator under COI reference	$TI_7 = \left\|f_i\right\| = \frac{\left\|P_{\mathrm{m}i}(t_{\mathrm{cl}}) - P_{ei}(t_{\mathrm{cl}}) - M_i \cdot P_{\mathrm{COI}}(t_{\mathrm{cl}})/M\right\|}{M_i}$
8	Maximum deviation of voltage magnitude of generator's integration bus	$TI_8 = \left\|V_i(t) - V_{iN}\right\|, t \in [t_{\mathrm{cl}}, t_{\mathrm{end}}]$
9	Accumulated effect of voltage deviation of generator's integration bus	$TI_9 = \int_{t_{\mathrm{cl}}}^{t_{\mathrm{end}}} \left\|V_i(t) - V_{iN}\right\| \mathrm{d}t$
10	Generator pair-wise potential energy [15]	$TI_{10} = \int_{t_{\mathrm{cl}}}^{t_{\mathrm{end}}} (\Delta P_{ei} - \Delta P_{ej})(\omega_i - \omega_j) \mathrm{d}t$
11	Maximum difference of accelerating power-rotor speed dot-product [16]	$TI_{11} = \max dot_1(t) - \min dot_1(t)$
12	Maximum difference of accelerating power-power angle dot-product [16]	$TI_{12} = \max dot_2(t) - \min dot_2(t)$
13	Maximum difference of rotor speed-power angle dot product [16]	$TI_{13} = \max dot_3(t) - \min dot_3(t)$

the delay of speed governors to adjust the mechanical power input, P_{m} is assumed to be similar to its pre-fault value; thus $P_{\mathrm{m}} \approx P_{\mathrm{m0}} = P_{\mathrm{e0}}$, and V can be directly measured by PMUs.

i, j are serial numbers of generators' integration buses while N_{G} is the amount of generators. t_{cl} is the clearance time of fault contingencies while t_{end} is the moment at which the observation window ends. The superscript of COI represents that the parameters are under the center of inertia (COI) reference. Here,

$$M = \sum_{i=1}^{N_{\mathrm{G}}} M_i, \quad \delta_{\mathrm{COI}} = \frac{1}{M} \sum_{i=1}^{N_{\mathrm{G}}} M_i \delta_i,$$
$$\omega_{\mathrm{COI}} = \frac{1}{M} \sum_{i=1}^{N_{\mathrm{G}}} M_i \omega_i, \quad P_{\mathrm{COI}} = \sum_{i=1}^{N_{\mathrm{G}}} (P_{\mathrm{m}i} - P_{ei})$$

where M_i is the inertia coefficient of the i^{th} generator and M is the aggregate inertia of all the generators in a system. For online application, inertia coefficient M_i can be estimated by parameter identification methods such as those proposed in [17].

V_{N} is rated value of the buses' voltage magnitude and $V_{\mathrm{N}} = 1$ when per unit value is adopted. ΔP_{e} is the difference of the generators' electrical power output with respect to pre-fault condition; thus $\Delta P_{\mathrm{e}} = P_{\mathrm{e}} - P_{\mathrm{e0}}$. Dot-products proposed in [16] are adopted in this paper and the definitions of these dot-products are given as follows:

$$dot_1 = f_i \cdot \omega_i^{\mathrm{COI}}$$
$$dot_2 = f_i \cdot \theta_i^{\mathrm{COI}}$$
$$dot_3 = \omega_i^{\mathrm{COI}} \cdot [\theta_i^{\mathrm{COI}} - \theta_i^{\mathrm{COI}}(t_{\mathrm{cl}})]$$

where

$$\delta_i^{\mathrm{COI}} = \delta_i(t) - \delta_{\mathrm{COI}}(t)$$
$$\omega_i^{\mathrm{COI}}(t) = \omega_i(t) - \omega_{\mathrm{COI}}(t)$$
$$f_i = \frac{P_{\mathrm{m}i}(t) - P_{ei}(t) - M_i \cdot P_{\mathrm{COI}}(t)}{M}.$$

Apart from the systematic indicators, TI_2 and TI_5, the other indicators reflect the post-fault response of each generator. Therefore, the maximum value, the average value, and the standard deviation of these indicators are utilized to evaluate the impact of fault contingencies on the post-fault system. These statistic value will be presented by max (TI_n), mean (TI_n), and std (TI_n) in this paper. Eventually, 35 indicators are proposed for transient stability assessment.

B. Correlation-based Indicator Selection

Among the aforementioned 35 indicators, some may not be effective for assessment. Thus indicator selection must be first conducted before fuzzy rule training and online assessment.

In order to verify the validities of transient indicators, a CCT-based stability *SI* is proposed. As is shown in (8), *SI* is a normalized margin index of fault clearance time with respect to CCT.

$$SI = \frac{t_{\mathrm{cr}} - t_{\mathrm{cl}}}{t_{\mathrm{cr}}} \tag{8}$$

Here, t_{cr} is CCT of a fault contingency while t_{cl} remains to be fault clearance time. Since CCT reflects the stability boundary of fault contingencies, *SI* is a valuable index for transient stability awareness. Iterative time domain simulations are necessary for computation of CCT, which makes it impractical to compute *SI* in real-time. However, by using correlation mining between *SI* and transient indicators, those indicators that are not sensitive to *SI* can be screened out. Thus the rest can be eventually selected as assessment criteria. Univariate regression is performed repeatedly to obtain the correlation functions between *SI* and indicators, as shown in (9):

$$SI = f_n(TI_n) + \varepsilon \tag{9}$$

where f_n represents the correlation function and ε denotes the regression error of this correlation function. Regression error of correlation functions can be evaluated through root mean square error (*RMSE*), as shown in (10):

$$RMSE_n = \sqrt{\frac{1}{S}\sum_{s=1}^{S}[SI_s - f_n(TI_{n,s})]^2} \tag{10}$$

where s is the serial number of samples, while S is the amount of samples. Indicators that have smaller *RMSE* are more sensitive to *SI*. Therefore, all the indicators can be ranked by *RMSE* and further selected for multi-indicator assessment.

Considering the different efficiencies of the selected indicators, weighting factor w_j can be allocated according to its regression error. The improved weighting factor can be computed by (11):

$$w_n = \frac{1/RMSE_n}{\sum_{n=1}^{N}(1/RMSE_n)}. \tag{11}$$

IV. Proposed Multi-indicator Inference Scheme

In this section, the proposed multi-indicators inference scheme for transient stability awareness is presented in detail.

A. Stage I: Data Preparation

Samples for indicator selection and fuzzy set division are generated through offline simulations on the platform proposed in [18]. A number of operating conditions (OCs) are first generated using stochastic load variations within 80% to 120% of base conditions. Transmission lines are chosen as fault elements of "$N-1$" three-phase fault contingencies and then TDSs of these contingencies under different OCs are executed to form a knowledge base. Post-fault responses within 10 cycles after fault clearance are utilized to compute all *TI* indicators. Meanwhile, the CCT and *SI* of each contingency are computed iteratively for critical contingency searching. *TI* and *SI* together compose a sample and all the samples are recorded in the knowledge base.

B. Stage II: Fuzzy Rule Training

Correlations between indicators and *SI* are first trained using univariate regression analysis with the knowledge base. The correlation functions and their regression error represented by *RMSE* are thus determined. Indicators are ranked according to *RMSE*s, and effective indicators are then selected for multi-indicator assessment. The weighting factors for the selected transient indicators are computed as in (11). Meanwhile, four fuzzy stability levels are defined: "safe," "low risk," "high risk," and "danger." These stability levels refer to four fuzzy sets of *SI*, which are [0.8, 1.0), [0.5, 0.8), [0.2, 0.5), and $(-\infty, 0.2)$. By computing the corresponding value of each selected indicator when *SI* takes value of 0.2, 0.5, 0.8, and 1.0, according to the correlation function, the fuzzy sets of different stability levels are then determined.

C. Stage III: Online Assessment

After a fault is cleared, post-fault PMU measurements within the observation window are utilized to compute all the transient indicators. Then the memberships of each indicator to different stability levels are computed according to the offline-trained fuzzy inference rule. Credibility measurement is then executed to assess the transient stability level of the post-fault system.

Fig. 1 demonstrates the procedure of the proposed multi-indicator inference scheme for transient stability awareness. It should be noted that the procedures surrounded by dashed line should be executed offline while the procedures surrounded by dot-dashed lines are applicable to either offline or online awareness of stability level.

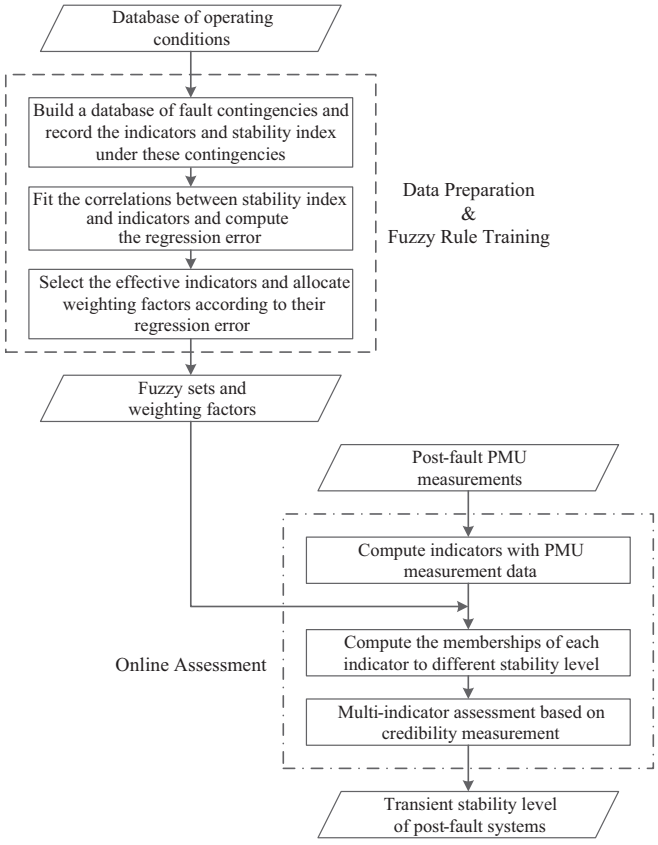

Fig. 1. Demonstration of the proposed scheme.

V. Illustrative Case Study on IEEE 68-bus System

A case study on the IEEE 68-bus system was conducted to illustrate the effectiveness of the proposed multi-indicator inference scheme. Training samples needed for fuzzy rule training were generated through offline TDSs according to Stage I of the proposed scheme. Two thousand (2000) samples were generated and the ones that were unstable within 10 seconds after fault clearance were screened out, while the stable ones were stored to form a knowledge base.

A. Correlation Mining and Indicator Selection

Univariate correlation mining between each indicator *TI* and stability index *SI* is performed to select effective indicators.

Polynomial functions and exponential function are used to fit the correlations respectively and the function with the least regression error is defined as the marginal correlation function. Fig. 2 shows the regression errors of all the marginal correlation functions. In order to reduce the redundancy of indicators, for each subset of indicators, such as $\{\max(TI_1), \text{mean}(TI_1), \text{std}(TI_1)\}$, only the one with the least regression error is chosen to compose the indicator set for further assessment. The selected indicators are highlighted in Fig. 2 and their correlation functions, regression errors, and weighting factors are shown in detail in Table II.

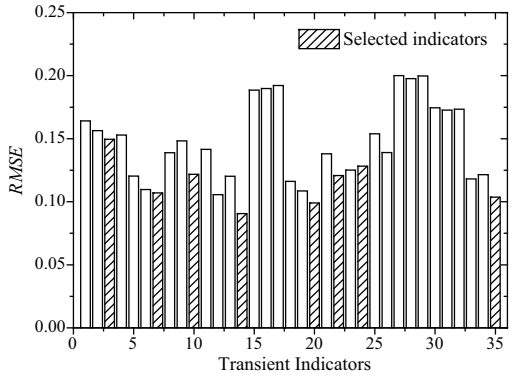

Fig. 2. Regression error *RMSE* of the correlation functions of transient indicators in IEEE 68-bus system case.

TABLE II
SELECTED TRANSIENT INDICATORS IN IEEE 68-BUS SYSTEM CASE

Indicators	Correlation Function	*RMSE*	Weighting Factor
Std (TI_1)	$f(x) = -3.8358x + 1.0510$	0.1495	0.0941
Std (TI_3)	$f(x) = 0.9919e^{-6.4884x}$	0.1070	0.1314
Std (TI_4)	$f(x) = -194.5679x - 6.4884$	0.1218	0.1155
Std (TI_6)	$f(x) = 0.9641e^{-52871x}$	0.0906	0.1552
Std (TI_8)	$f(x) = 0.9778e^{-24.6902x}$	0.0991	0.1420
Mean (TI_9)	$f(x) = 0.8602e^{-27.6847x}$	0.1208	0.1164
Max (TI_{10})	$f(x) = 0.7867e^{-10.7101x}$	0.1283	0.1097
Std (TI_{13})	$f(x) = 0.9230e^{-1100.3x}$	0.1037	0.1357

Figs. 3–10 are scatter diagrams of fault contingency samples under coordinates of each indicator and *SI*, respectively. Although all the indicators are sensitive to responses of different fault contingencies, negative correlation exists between each indicator and *SI*.

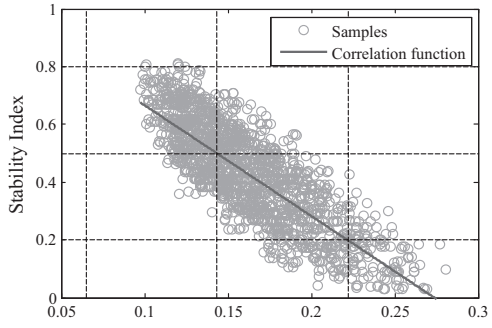

Fig. 3. Scatter diagram of fault contingency samples and the correlation curve between stability index SI and the standard deviation index of the 1^{st} transient indicator std (TI_1).

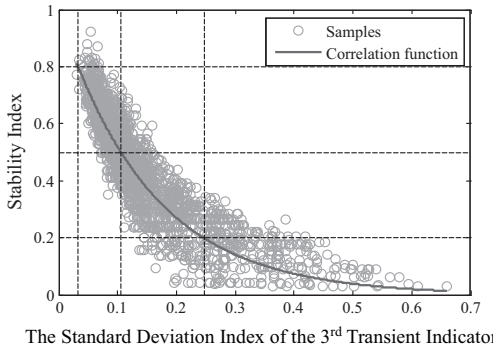

Fig. 4. Scatter diagram of fault contingency samples and the correlation curve between stability index SI and the standard deviation index of the 3^{rd} transient indicator std (TI_3).

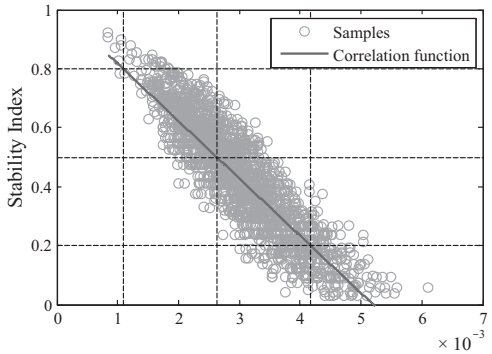

Fig. 5. Scatter diagram of fault contingency samples and the correlation curve between stability index SI and the standard deviation index of the 4^{th} transient indicator std (TI_4).

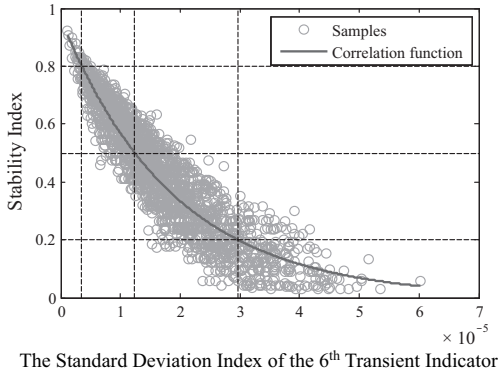

Fig. 6. Scatter diagram of fault contingency samples and the correlation curve between stability index SI and the standard deviation index of the 6^{th} transient indicator std (TI_6).

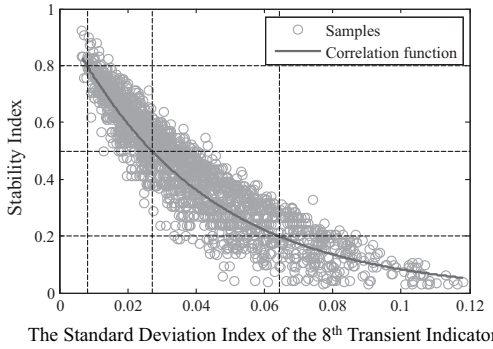

Fig. 7. Scatter diagram of fault contingency samples and the correlation curve between stability index SI and the standard deviation index of the 8^{th} transient indicator std (TI_8).

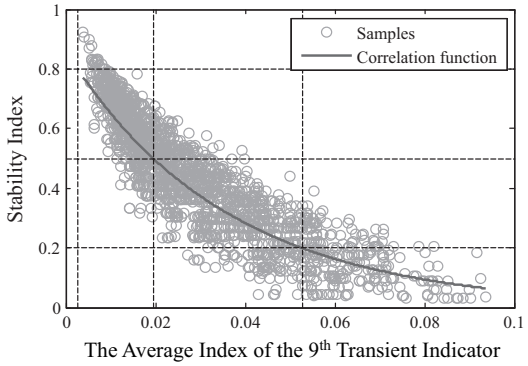

Fig. 8. Scatter diagram of fault contingency samples and the correlation curve between stability index SI and the average index of the 9^{th} transient indicator mean (TI_9).

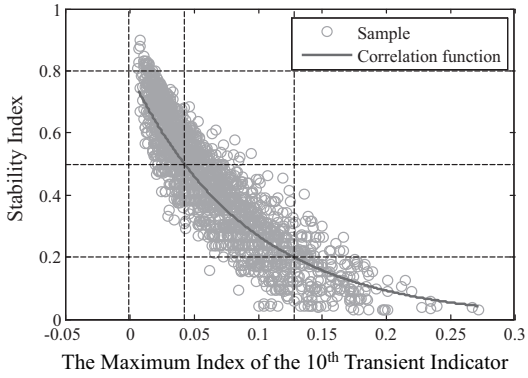

Fig. 9. Scatter diagram of fault contingency samples and the correlation curve between stability index SI and the standard deviation index of the 10^{th} transient indicator std (TI_{10}).

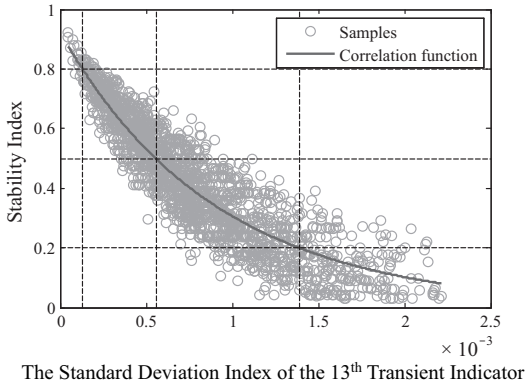

Fig. 10. Scatter diagram of fault contingency samples and the correlation curve between stability index SI and the standard deviation index of the 13^{th} transient indicator std (TI_{13}).

B. Computation of Fuzzy Sets

Four fuzzy stability levels, "safe," "low risk," "high risk," and "danger," are defined for fuzzy inference of transient stability level. By computing the corresponding value of each selected indicator when *SI* takes value of 0.2, 0.5, 0.8, and 1.0, according to the correlation function, the fuzzy sets of all the indicators are thereby determined. The fuzzy sets of all the indicators in IEEE 68-bus system case are given in Table III.

TABLE III
FUZZY SETS OF TRANSIENT INDICATORS IN IEEE 68-BUS SYSTEM CASE

Indicators	Safe	Low-Risk	High-Risk	Danger
TI_2	0.013–0.065	0.065–0.144	0.144–0.222	0.222–0.274
Mean (TI_3)	0.000–0.033	0.033–0.106	0.106–0.247	0.247–1.418
Std (TI_4)	0.000–0.001	0.001–0.003	0.003–0.004	0.004–0.005
Std (TI_6)	0.000–0.035	0.035–0.124	0.124–0.297	0.297–1.735
Std (TI_8)	0.000–0.008	0.008–0.027	0.027–0.064	0.064–0.372
Mean (TI_9)	0.000–0.003	0.003–0.020	0.020–0.053	0.053–0.327
Max (TI_{10})	−0.022–−0.002	−0.002–0.042	0.042–0.128	0.128–0.838
Max (TI_{13})	0.000–0.130	0.130–0.557	0.557–1.390	1.390–8.298

C. Online Awareness of Transient Stability Level of Fault Contingencies

Under the same operating condition of IEEE 68-bus system, 5 three-phase fault contingencies are chosen as testing samples for validation of the proposed fuzzy assessment scheme. Results of the indicators and fuzzy assessment of transient stability are shown in Table IV and Table V separately. Also, Fig. 11 further demonstrates visually the transient stability

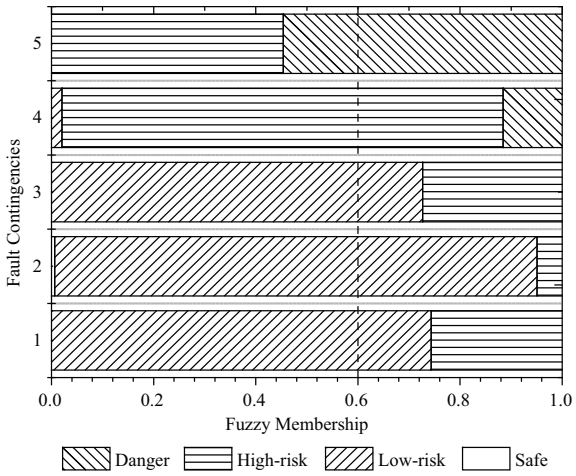

Fig. 11. Demonstration of credibility assessment of transient stability level of different fault contingencies in IEEE 68-bus system case.

TABLE IV
TRANSIENT INDICATORS OF DIFFERENT FAULT CONTINGENCIES IN IEEE 68-BUS SYSTEM CASE

Fault Contingency	t_{cl} (s)	t_{cr} (s)	Std (TI_1)	Std (TI_3)	Std (TI_4)	Std (TI_6)	Std (TI_8)	Mean (TI_9)	Max (TI_{10})	Std (TI_{13})
2[a]–25	0.10	0.28	0.1355	0.0683	0.0020	1.3579	0.0135	0.0077	0.0155	0.7343
15[a]–16	0.10	0.34	0.1256	0.0652	0.0017	0.6930	0.0197	0.0129	0.0149	0.3670
16[a]–21	0.10	0.23	0.1240	0.0721	0.0022	1.3100	0.0175	0.0134	0.0220	0.7540
14[a]–15	0.25	0.38	0.1548	0.1947	0.0034	2.0900	0.0579	0.0462	0.0964	0.9850
17[a]–18	0.25	0.30	0.1842	0.2921	0.0041	3.6000	0.0555	0.0554	0.1072	1.8740

[a] represents that short-circuit fault locates near to the marked bus.

TABLE V
FUZZY ASSESSMENT OF TRANSIENT STABILITY LEVEL OF DIFFERENT FAULT CONTINGENCIES IN IEEE 68-BUS SYSTEM CASE

Fault Contingency	*SI*	Safe	Low-risk	High-risk	Danger	Stability Level
2[a]–25	0.6429	0.0000	0.7435	0.2565	0.0000	Low-risk
15[a]–16	0.7059	0.0063	0.9444	0.0493	0.0000	Low-risk
16[a]–21	0.5652	0.0000	0.7267	0.2733	0.0000	Low-risk
14[a]–15	0.3421	0.0000	0.0203	0.8641	0.1156	High-risk
17[a]–18	0.1667	0.0000	0.0000	0.4540	0.5460	Danger

[a] represents that short-circuit fault locates near to the marked bus.

level according to credibility assessment. As seen in Table V and Fig. 11, the proposed fuzzy inference scheme is able to achieve a fuzzy assessment of transient stability level within 10 cycles after fault clearance, and the assessment results agree with *SI*.

VI. APPLICATION TO A PRACTICAL TRANSMISSION SYSTEM

The 500 kV bulk network of a large-scale transmission system in China is shown in Fig. 12. This system consists of 756 buses (500 kV buses, 220 kV buses and low-voltage generators' terminal buses), 630 transmission lines, 449 transformers and 135 generators. High-order dynamic models for synchronous generators, turbines, speed governors, excitation systems, and power system stabilizers are utilized for simulation. Similarly, with the previous case, correlation mining is first performed to select effective indicators. Fig. 13 shows the regression errors of all the marginal correlation functions, and the correlation functions, regression errors, and weighting factors of the selected indicators are shown in Table VI.

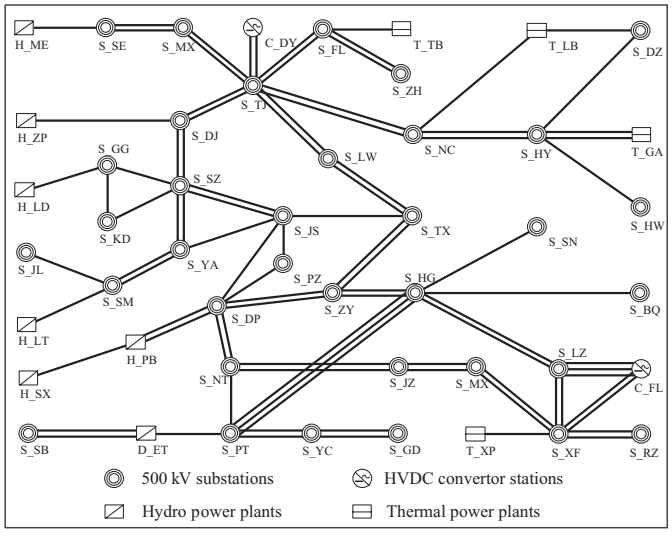

Fig. 12. 500 kV bulk network of a practical transmission system.

The fuzzy sets of these selected transient indicators are also computed according to their correlation functions to *SI* and are given in Table VII.

In the case study on the practical 756-bus transmission system, 5 fault contingencies are chosen as testing samples for validation of the proposed multi-indicator inference scheme. Table VIII and Table IX present the assessment results of these fault contingencies. Meanwhile, Fig. 14 demonstrates the transient stability level according to credibility assessment. It is clear that the assessment agrees with *SI*, demonstrating that the selected indicators are able to quantify the impacts of faults on power systems and that fast assessment of transient stability level can be achieved by the proposed scheme.

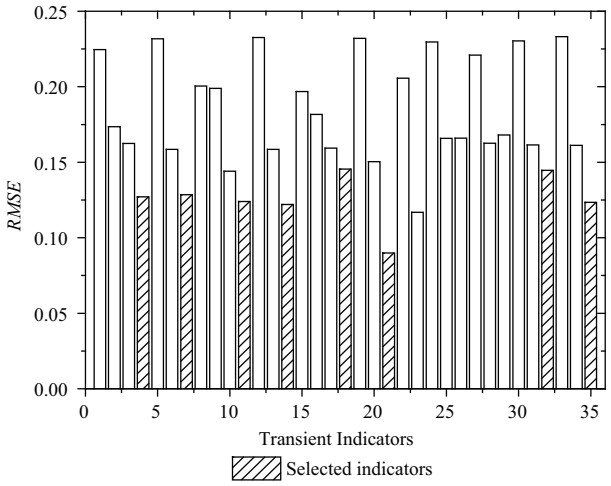

Fig. 13. Regression error *RMSE* of the correlation functions of transient indicators in practical transmission system case.

TABLE VI
THE SELECTED TRANSIENT INDICATORS IN PRACTICAL TRANSMISSION SYSTEM CASE

Indicators	Correlation Function	*RMSE*	Weighting Factor
TI_2	$f(x) = 2.9698e^{-1.2203x}$	0.1271	0.1220
Std (TI_3)	$f(x) = 1.2101e^{-4.9370x}$	0.1285	0.1207
TI_5	$f(x) = -0.1030x + 1.0245$	0.1241	0.1250
Std (TI_6)	$f(x) = 0.8291e^{-0.4390x}$	0.1220	0.1271
Max (TI_8)	$f(x) = 1.3037e^{-3.7782x}$	0.1551	0.1000
Max (TI_9)	$f(x) = 0.9499e^{-5.7787x}$	0.0899	0.1724
Std (TI_{12})	$f(x) = -31.1592x + 0.8134$	0.1447	0.1072
Std (TI_{13})	$f(x) = 0.8273e^{-2.9629x}$	0.1234	0.1256

TABLE VII
FUZZY SETS OF TRANSIENT INDICATORS IN PRACTICAL TRANSMISSION SYSTEM CASE

Indicators	Safe	Low-risk	High-risk	Danger
TI_2	0.892–1.075	1.075–1.460	1.460–2.211	2.211–8.439
Std (TI_3)	0.039–0.084	0.084–0.179	0.179–0.365	0.365–1.904
TI_5	0.239–2.180	2.180–5.094	5.094–8.007	8.007–9.949
Std (TI_6)	0.0–0.081	0.081–1.152	1.152–3.239	3.239–20.553
Max (TI_8)	0.070–0.129	0.129–0.254	0.254–0.496	0.496–2.508
Max (TI_9)	0.0–0.030	0.030–0.111	0.111–0.270	0.270–1.585
Std (TI_{12})	0.0–4.29E-4	4.29E-4–0.010	0.010–0.026	0.020–0.026
Std (TI_{13})	0.0–0.011	0.011–0.170	0.170–0.479	0.479–3.045

TABLE VIII
FUZZY ASSESSMENT OF TRANSIENT STABILITY OF PRE-DEFINED FAULT CONTINGENCIES IN PRACTICAL TRANSMISSION SYSTEM CASE

Fault Contingency	t_{cl} (s)	t_{cr} (s)	TI_2	Std (TI_3)	TI_5	Std (TI_6)	Max (TI_8)	Max (TI_9)	Std (TI_{12})	Std (TI_{13})
T_LB[a]-NC	0.2	0.31	1.7228	0.2445	7.9910	5.8752	0.3755	0.2469	0.0181	0.8302
PT[a]-H_ET	0.2	0.45	1.2427	0.1264	4.2575	0.9018	0.2375	0.0810	0.0039	0.0876
SZ-JS	0.2	0.57	1.4759	0.1907	4.6860	0.7804	0.2585	0.0780	0.0046	0.1135
DP[a]-H_PB	0.2	0.71	1.3018	0.1501	2.7156	0.3107	0.0903	0.0211	0.0012	0.0426
YA[a]-SZ[a]	0.4	0.57	2.2220	0.2620	5.7340	3.4876	0.2757	0.1582	0.0115	0.5977

[a] represents that short-circuit fault locates near to the marked bus.

TABLE IX
FUZZY ASSESSMENT OF TRANSIENT STABILITY LEVEL OF DIFFERENT FAULT CONTINGENCIES IN PRACTICAL TRANSMISSION SYSTEM CASE

Fault Contingency	*SI*	Safe	Low-risk	High-risk	Danger	Stability Level
T_LB[a]-NC	0.3548	0.0000	0.0000	0.6070	0.3930	High-risk
PT[a]-H_ET	0.5556	0.0000	0.8800	0.1200	0.0000	Low-risk
SZ[a]-JS	0.6491	0.0000	0.7063	0.2937	0.0000	Low-risk
DP[a]-H_PB	0.7183	0.3102	0.6552	0.0346	0.0000	Low-risk
YA[a]-SZ	0.2982	0.0000	0.1048	0.6427	0.2525	High-risk

[a] represents that short-circuit fault locates near to the marked bus.

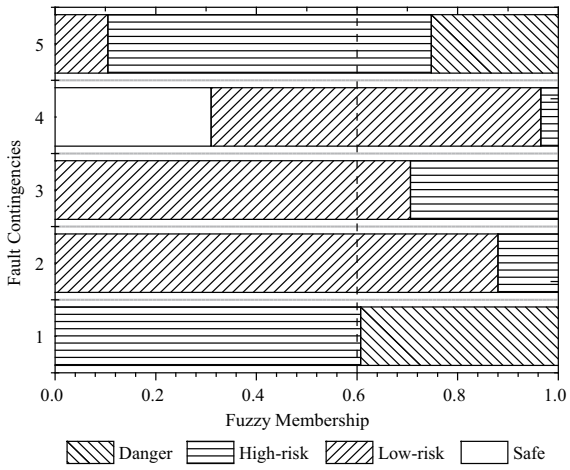

Fig. 14. Demonstration of credibility assessment of transient stability level of different fault contingencies in practical transmission system case.

VII. CONCLUSION

A multi-indicator fuzzy inference scheme is proposed to achieve comprehensive assessment of post-fault transient stability of power systems. A multi-criteria quality assessment method is first introduced. Thirteen types of transient indicators are then defined for evaluating the severity of fault contingencies. A correlation-based feature selection method is further proposed to select the effective indicators for stability assessment. By successively univariate regression analysis between transient indicators and a critical clearance time-based stability index *SI* and regression error ranking, the indicators that are sensitive to *SI* are chosen as assessment criteria. Also, the weighting factors for all the selected indicators are allocated according to the regression error of their correlation functions to *SI*. Four fuzzy stability levels, "safe," "low-risk," "high-risk," and "danger" are defined based on *SI*, and the corresponding fuzzy sets for transient indicators are computed according to their correlation functions. The proposed inference scheme is then demonstrated and its effectiveness is validated via case studies on IEEE 68-bus system and a practical 756-bus transmission system in China.

REFERENCES

[1] IEEE/CIGRE Joint Task Force on Stability Terms and Definitions, "Definition and classification of power system stability," *IEEE Transactions on Power Systems*, vol. 19, no. 2, pp. 1387–1401, May 2004.

[2] J. Q. Lv, M. Pawlak, and U. D. Annakkage. "Prediction of the transient stability boundary using the lasso," *IEEE Transactions on Power Systems*, vol. 28, no. 1, pp. 281–288, Feb. 2013.

[3] M. He, V. Vittal, and J. S. Zhang. "Online dynamic security assessment with missing PMU measurements: a data mining approach," *IEEE Transactions on Power Systems*, vol. 28, no. 2, pp. 1969–1977, May 2013.

[4] M. He, J. S. Zhang, and V. Vittal. "Robust online dynamic security assessment using adaptive ensemble decision-tree learning," *IEEE Transactions on Power Systems*, vol. 28, no. 4, pp. 4089–4098, Nov. 2013.

[5] C. X. Liu, K. Sun, Z. H. Rather, Z. Chen, C. L. Bak, P. Thøgersen, and P. Lund. "A systematic approach for dynamic security assessment and the corresponding preventive control scheme based on decision trees," *IEEE Transactions on Power Systems*, vol. 29, no. 2, pp. 717–730, Mar. 2014.

[6] A. D. Rajapakse, F. Gomez, K. Nanayakkara, P. A. Crossley, and V. V. Terzija, "Rotor angle instability prediction using post-disturbance voltage trajectories," *IEEE Transactions on Power Systems*, vol. 25, no. 2, pp. 947–956, May 2010.

[7] F. Gomez, A. D. Rajapakse, U. D. Annakkage, and I. T. Fernando. "Support vector machine-based algorithm for post-fault transient stability status prediction using synchronized measurements," *IEEE Transactions on Power Systems*, vol. 26, no. 3, pp. 1474–1483, Aug. 2011.

[8] J. Geeganage, U. D. Annakkage, T. Weekes, and B. A. Archer. "Application of energy-based power system features for dynamic security assessment," *IEEE Transactions on Power Systems*, vol. 30, no. 4, pp. 1957–1965, Jul. 2015.

[9] T. Amraee and S. Ranjbar. "Transient instability prediction using decision tree trchnique," *IEEE Transactions on Power Systems*, vol. 28, no. 3, pp. 3028–3037, Aug. 2013.

[10] S. K. Tso, L. Guan, Q. Y. Zeng, and K. L. Lo. "Fuzzy assessment of power system transient stability level based on steady-state data," *IET proceedings in Generation, Transmission and Distribution*, vol. 144, no. 6, pp. 525–531, Nov. 1997.

[11] J. M. Alvarez and P. E. Mercado, "Online inference of the dynamic security level of power systems using fuzzy techniques," *IEEE Transactions on Power Systems*, vol. 22, no. 2, pp. 717–726, May. 2007.

[12] T.-J. Liu, J.-Y. Liu, Y.-B. Liu, J.-S. Yang, and Y.-Q. Ni. "Multi-performance criteria evaluation for severe disturbance screening regarding transient impacts," in *2014 International Conference on Power System Technology (POWERCON)*, Chengdu, China, pp. 594-600.

[13] G. Li and S. M. Rovnyak, "Integral square generator angle index for stability ranking and control," *IEEE Transactions on Power Systems*, vol. 20, no. 2, pp. 926–934, May. 2005.

[14] I. Kamwa, J. Beland, and D. McNabb. "PMU-based vulnerability assessment using wide-area severity indices and tracking modal analysis," in *IEEE PES Power Systems Conference and Exposition*, 2006, pp. 139–149.

[15] C. S. Saunders, M. M. Alamuti, and G. A. Taylor. "Transient stability analysis using potential energy indices for determining critical generator sets," in *IEEE PES General Meeting*, 2014, pp. 1–5.
[16] C. J. Fu and A. Bose, "Contingency ranking based on severity indices in dynamic security analysis," *IEEE Transactions on Power Systems*, vol. 14, no. 3, pp. 980–986, Aug. 1999.
[17] Y. C. Zhang, J. Bank, E. Muljadi, Y.-H. Wan, and D. Corbus. "Angle instability detection in power systems with high-wind penetration using synchrophasor measurements," *IEEE Journal of Emerging and Selected Topics in Power Electronics*, vol. 1 no. 4, pp. 306–314, Dec. 2013.
[18] Y. B. Liu, Y. Liu, J. Y. Liu, C. S. Saunders, G. A. Taylor, B. Masoud and W. X. Liang. "A cloud computing framework for cascading failure simulation and analysis of large-scale transmission systems," in *2014 International Conference on Power System Technology (POWERCON)*, 2014, pp. 287–293.

Tingjian Liu received his B.S. degree in electrical engineering from Sichuan University, Chengdu, China, in 2013. Currently, he is a graduate student in the School of Electrical Engineering and Information, Sichuan University. His research interests include transient stability analysis of power systems and the application of big-data technologies in power systems.

Youbo Liu (M'13) received his Ph.D. degree from School of Electrical Engineering and Information, Sichuan University, Chengdu, China, in 2011. He is a Lecturer in the School of Electrical Engineering and Information, Sichuan University. His research interests include cascading failures and vulnerability analysis, power system big-data application.

Junyong Liu received his Ph.D. degree from the School of Engineering and Design, Brunel University, UK, in 1997. He is a Professor with the School of Electrical Engineering and Information, Sichuan University, Chengdu, China. His current research interests include intelligent dispatch and operation theory for smart grids. He was a Distinguished Visiting Fellow of Brunel University, London, UK, funded by the Royal Academy of Engineering.

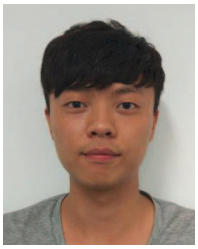

Yue Yang received his B.S. degree in electrical engineering from Sichuan University, Chengdu, China, in 2015. He is a graduate student in the School of Electrical Engineering and Information, Sichuan University. His research interests include application of data mining technologies in transient stability analysis.

Gareth A. Taylor (M'09–SM'12) received his B.Sc. degree from the University of London, London, U.K., in 1987, and the M.Sc. and Ph.D. degrees in power systems from the University of Greenwich, London, in 1992 and 1997, respectively. He was the National Grid U.K. Post-Doctoral Scholar at Brunel University, London, from 2000 to 2003. He is currently a Professor and Director within the Brunel Institute of Power Systems, Brunel University, London. His current research interests include smart grids, wide area monitoring of power systems, and network optimization.

Zhengwen Huang received the Ph.D. degree from the Department of Electronic and Computer Engineering at Brunel University, London, UK. Currently, he is a Research Fellow in the Brunel Institute of Power Systems, Brunel University. His research interests include evolutionary algorithms and data engineering.